Scanning Microscopy

Volume 9 | Number 1 Article 3

2-20-1995

Investigation of Nanoparticles in High Resolution Scanning Electron Microscopy (SEM) and Low Voltage SEM by Digital Image-Analysis

B. Ocker
Universitat Hohenheim

R. Wurster
Universitat Hohenheim

H. Seiler
Universitat Hohenheim

Scanning Microscopy, Vol. 9, No. 1, 1995 (Pages 63-73) 0891-7035/95$5.00+.25
Scanning Microscopy International, Chicago (AMF O'Hare), IL 60666 USA

INVESTIGATION OF NANOPARTICLES IN HIGH RESOLUTION SCANNING ELECTRON MICROSCOPY (SEM) AND LOW VOLTAGE SEM BY DIGITAL IMAGE-ANALYSIS

B. Ocker*, R. Wurster and H. Seiler

Institut für Physik, Universität Hohenheim,
Garbenstrasse 30, D-70599 Stuttgart, Germany

(Received for publication April 18, 1994 and in revised form February 20, 1995)

Abstract

Small particles (Cu, Ag, In, Sn, Au, also MgO and NaCl) were prepared in the diameter range from 1 nm to 100 nm on different conductive substrates by thermal evaporation in high-vacuum or in an inert gas atmosphere. Imaging of the particles was performed in a high resolution scanning electron microscope (HRSEM) that can also be operated at low beam voltages of a few hundred volts. This mode of operation is called low voltage SEM (LVSEM). Scanning electron micrographs were taken at different beam voltages V_0 (0.5-30 kV). The micrographs were digitally recorded and analyzed with an image processing system operated on-line to the HRSEM. Grey-value line profiles and densitometric quantities of single particles, as well as the contrast between particle and substrate, changed with V_0. The results for tin-particles on a bulk carbon substrate are shown. In all cases considered, only positive contrasts, i.e., particles looking brighter than the substrate, were obtained. The main contrast producing mechanism is, therefore, assigned to effects that include the particle's geometrical properties of size, shape and surface.

Sn-, In-, and Ag-particles, imaged in the secondary electron (SE) mode showed significantly larger particle diameters, as did images simultaneously recorded with transmitted electrons; however, Au-particles did not show that difference. This effect may be qualitatively explained by SE resulting from decaying plasmons.

Key words: High resolution scanning electron microscopy (HRSEM), low voltage SEM, scanning transmission electron microscope, digital image analysis, nanoparticles, topographic contrast, particle-to-substrate contrast.

*Address for correspondence:
B. Ocker, address as above.
Telephone number: (49) 711-459 2151
FAX number: (49) 711-459 2461

Introduction

Ultrafine particles with diameters less than 0.1 μm are of an ever increasing interest, particularly in material sciences and the industrial production of powder catalysts, ceramics, electronic devices, etc. Basic investigations, as well as applied research on nanoparticles, rely on a variety of sophisticated instrumentation, including electron microscopes of a sufficient resolving power. Without the time-consuming preparation techniques used in transmission electron microscopy, the surface and topography of bulk specimens can be imaged by high resolution scanning electron microscopes (HRSEM) at resolutions approaching 1 nm (Seiler and Bauer, 1989; Joy, 1991). This high performance in SEMs is achieved by utilizing field emission electron sources and highly excited objective lenses, and with the samples positioned in-lens. Recently, a similar performance was reported for a SEM with a new immersion type of objective lens that uses the combined effect of a magnetic and electrostatic field (Lanio *et al.*, 1993). For critical dimension measurements, e.g., the determination of the width of wells and trenches in integrated circuits, careful analysis and sufficient theoretical understanding of video signal linescans are indispensable prerequisites. The commonly used method for this purpose are based on the Monte Carlo simulation of electron trajectories and the calculation of secondary electron (SE) and backscattered electron (BSE) intensity profiles as a function of specimen and electron beam related parameters (see, e.g., Kotera *et al.*, 1993). Similar problems and questions arise, e.g., in the case of spherical nanoparticles on a smooth and polished substrate. As there seems to be a lack of experimental data in the literature, we have produced and deposited metallic nanoparticles on substrates of different elemental compositions. Using a digital image analysis system, the HRSEM images have been quantitatively evaluated in terms of particle-to-substrate contrasts and digital grey-level linescans across the centers of the particles. A qualitative interpretation of the results is based on the size and shape of the interaction volume and the information depth for SE and BSE emissions.

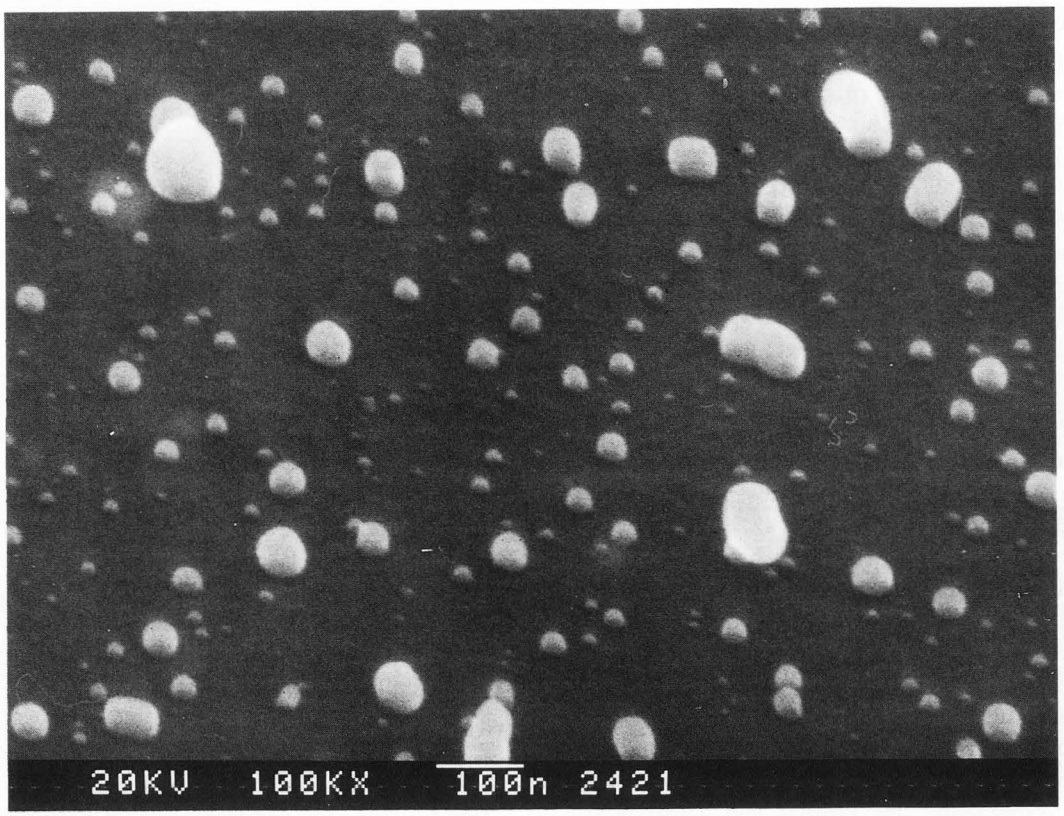

Figure 1. Micrograph of tin particles on bulk carbon, V_o = 20 kV, tilt angle 60°; bar = 100 nm.

Materials and Methods

Particle generation

Metallic particles were produced by thermal evaporation of metals either in high vacuum (appropriate for In, Sn, Au) or in an inert gas atmosphere of about 100 Pa N_2, Kr or He (appropriate for many materials, e.g., Cu, Ag, In, Sn, Au) (Ocker, 1993). Three different substrates used were: thin carbon foils, amorphous bulk carbon, and polished metal surfaces. The particle deposition was homogeneous all over the substrate's surface (3 mm x 3 mm). The amount of the deposited material was monitored by a piezoelectric balance. Depending on the experimental parameters, the diameters of the spherical to semi-spherical particles can be adjusted to 1 to 100 nm.

For high vacuum evaporation, the substrate was positioned at a distance of 15 cm above the evaporation source. The experimental parameters were: evaporation speed (source temperature), evaporation time (influences the amount of material on substrate), substrate temperature, and substrate material. In high vacuum, single atoms reach the substrate, and processes of nucleation and diffusion on its surface lead to production of discontinuous films and the growth of three-dimensional islands and particles. This process strongly depends on the mobility of the atoms. If the amount of impacted material is too large or the substrate is too cold, a homogeneous film is soon formed. An example is presented later in Figure 6a (tin particles on a carbon foil).

For evaporation process in an inert gas atmosphere, the important parameters determining the result are: source temperature, kind of gas, gas pressure, gas temperature, and distance between substrate and source. Collisions between metal and gas atoms induce condensation and particle generation within a distance of only a few millimeters from the vapor source that must be heated to temperatures well beyond the boiling point of the material. In the gas borne state, the particles can also increase by collisions with other particles. Only particles of a close size distribution range reach the substrate. Figures 1, 2a, 3a, and 4a show scanning electron micrographs of tin particles on bulk carbon. The particles have been generated in 60 Pa Kr atmosphere, the substrate to source distance was about 10 cm and the amount of tin on the substrate was equivalent to a homogeneous foil of 10 nm.

The high resolution SEM (HRSEM)

For characterization of particle samples, we used a

high resolution and low-voltage SEM (ABT DS 150F, Topcon, Tokyo, Japan). It is equipped with a thermal Schottky field emitting gun (TSFEG). At accelerating voltages (V_o) of 25-30 kV, this instrument has a nominal lateral resolution of about 1 nm (using SE detection). To obtain this high resolving power, the specimen must be placed between the pole pieces of a highly excited, short working distance objective ("in-lens" position). As the magnetic field of the lens operates as a conductor and collector, the SE can be detected by the usual scintillator-multiplier combination, mounted outside the lens, a few centimeters to the electron optical axis. This method efficiently suppresses the detection of BSE. In other words, the major part of the detector signal is caused by SE(1) and SE(2) secondary electrons, the latter generated by BSE in the specimen surface (Seiler, 1983). V_o can be varied between 0.5 kV and 30 kV. At a beam voltage of 1 kV, the resolution limit deteriorates to about 4 nm.

A detector for transmitted electrons (TE) is placed behind the objective lens and the specimen stage. It can be used with beam voltages $V_o > 13$ kV and for sufficiently thin objects. In this case, a simultaneous detection of reasonable SE and TE signals is possible.

A second specimen chamber below a second objective lens allows the investigation of samples not restricted in size (contrary to in-lens position) and at increased resolution limits (Ocker *et al.*, 1992a).

The image analysis system

A digital image analysis system SEM-IPS (Kontron, Munich, Germany) is connected to the HRSEM. The different detector signals, having been electronically amplified (visual image contrast) and leveled up or down (image brightness), are acquired on-line by the SEM-IPS and stored digitally in a video memory (e.g., at 512 x 512 pixels, 8 bit grey-value resolution). The digital equivalent of the scanning electron micrograph can be observed on an image display of the image analysis system. Besides a qualitative visual interpretation, the images can be quantitatively analyzed in terms of various object specific and densitometric features (e.g., particle diameter, brightness, contrast) by applying the appropriate programs of an extensive image processing software package. Single picture elements (pixels), any type of line-scans, and arbitrarily shaped picture areas are accessible for direct measurements.

Definition of grey-values and contrast

During the acquisition of a 512 x 512 pixel image, the video signals given by the detector are assigned grey-values from 0 to 255 (8 bit) by a linear analog to digital (A/D) conversion. Thus, an image is defined by a set of voltages (U_{min}, U_{max}) and grey-values (0 ... 255). For visual inspection and analysis, the digitized image can be displayed as a grey-tone picture as well as pseudocolored.

By blanking the primary electrons beam for a short interval during image acquisition, the grey-value scale becomes independent of those offset voltages, that can be arbitrary added or subtracted to the SEMs video amplifier voltage (brightness). The contrast (C) between a single particle and the substrate is calculated according to:

$$C = \{(GV_p - GV_s) / (GV_p + GV_s)\} \qquad (1)$$

where GV_p and GV_s are the mean values of all grey-values within the borders of the considered particle and a reference area on the substrate, respectively. The reference area was carefully selected in order to include a representative part of the substrate.

Results and Discussion

Estimation of the most useful accelerating voltage

Figures 2a, 3a, and 4a show micrographs of tin particles on bulk carbon taken at V_o = 1.5, 6, and 25 kV, respectively, at a magnification of 100,000x. In order to avoid visible electron beam induced effects, such as contamination layers and specimen damages, we had to choose a new area on the specimen for each micrograph.

At 1.5 kV and 25 kV, most of the particles appear brighter at their rims, whereas at 6 kV, the centers of the particles are the brightest. For particles in the diameter range observed, this effect appeared at V_o between 3 kV and 15 kV; for $V_o < 3$ kV and $V_o > 15$ kV, an enhanced edge brightness of the particles was again observed.

Figures 2b, 3b, and 4b, show scatter plots of the measured mean brightness (the mean grey-value) of single particles depending on their projected area diameters for the beam voltages 1.5 kV, 6 kV, and 25 kV, respectively; the mean grey-values of the substrates (GV_s) are also provided in the figure legends.

At 1.5 kV (Fig. 2b), the brightness increases fairly linearly until the particle diameters reach 50-60 nm. At higher diameter values, however, a slight decrease in particle brightness seems to arise. At 6 kV (Fig. 3b), the brightness continues to increase with particle diameters on the sample. For particles with diameters > 40 nm, the increase is stronger than for the smaller particles. At 25 kV (Fig. 4b), the brightness shows a similar course as at 6 kV. Similar effects have been observed for particles deposited onto bulk metallic or thin foil substrates (results not shown here).

Figures 2c, 3c, and 4c show grey-value linescans through the centers of some particles taken from the corresponding digitized scanning electron micrographs (Figs. 2a, 3a, and 4a). These linescans clearly and

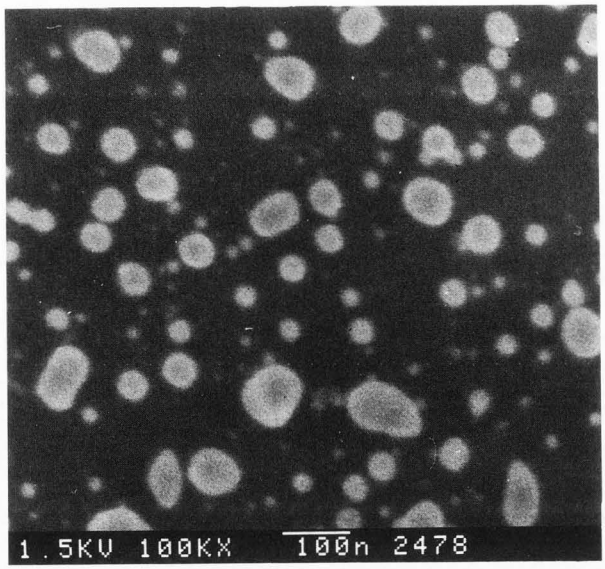

Figure 2a. Micrograph of tin particles on bulk carbon, V_o = 1.5 kV. Bar = 100 nm.

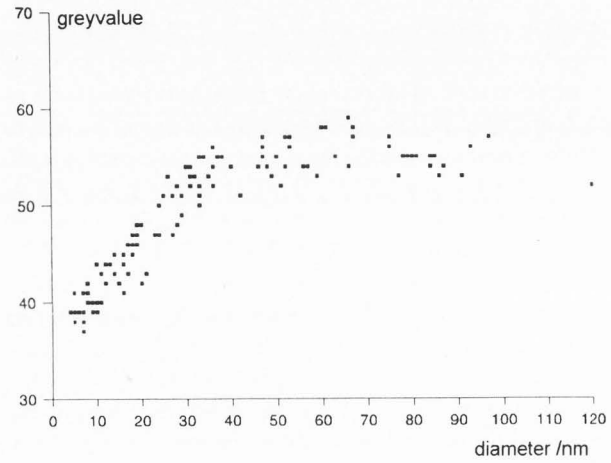

Figure 2b. Mean grey-values at V_o = 1.5 kV, GV(substrate) = 32.

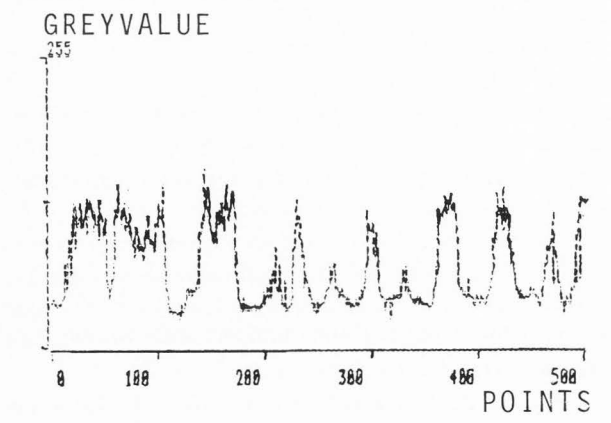

Figure 2c. Linescans through the centers of some particles of Figure 2a; 100 points ≡ 100 nm.

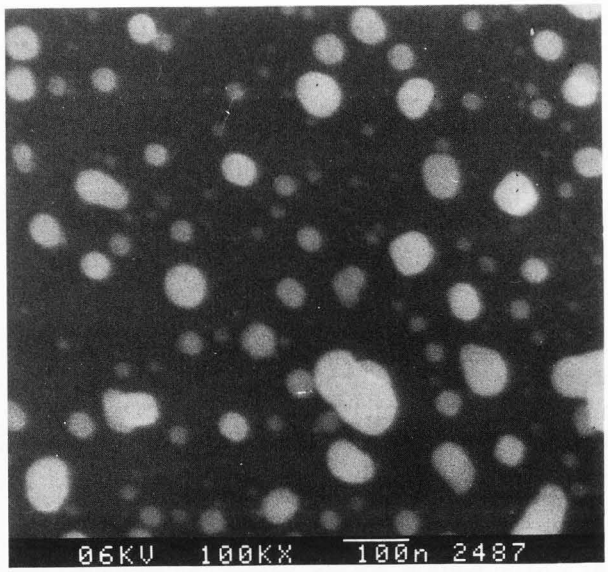

Figure 3a. Micrograph of tin particles on bulk carbon, V_o = 6 kV. Bar = 100 nm.

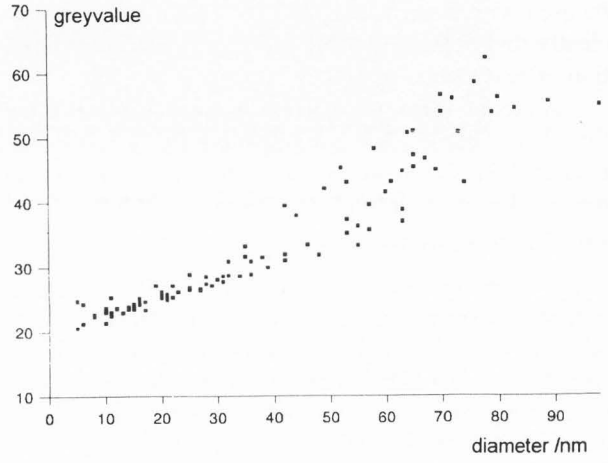

Figure 3b. Mean grey-values at V_o = 6 kV, GV(substrate) = 15.

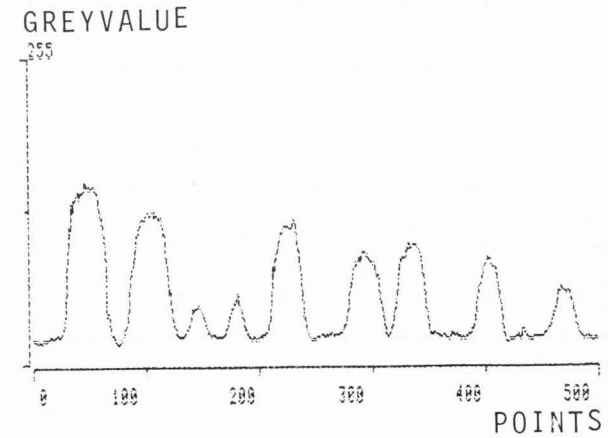

Figure 3c. Linescans through the centers of some particles of Figure 3a; 100 points ≡ 100 nm.

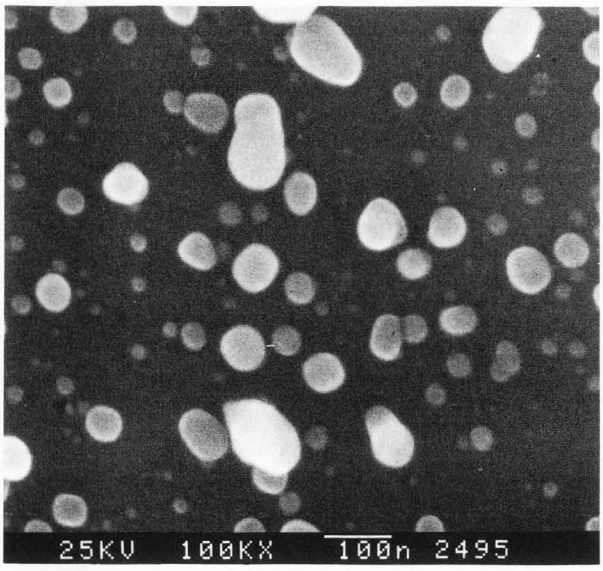

Figure 4a. Micrograph of tin particles on bulk carbon, V_o = 25 kV. Bar = 100 nm.

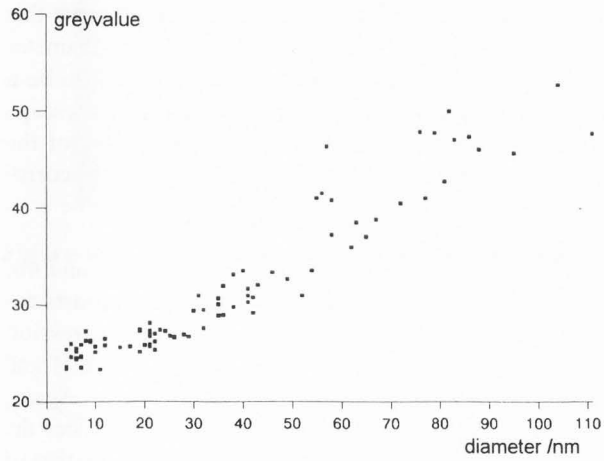

Figure 4b. Mean grey-values at V_o = 25 kV, GV(substrate) = 20.

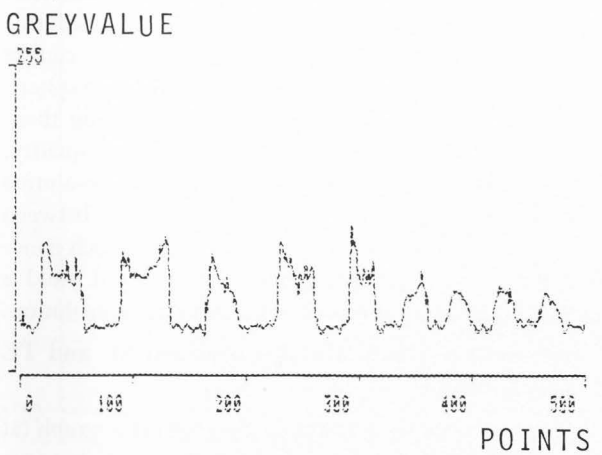

Figure 4c. Linescans through the centers of some particles of Figure 4a; 100 points ≡ 100 nm.

quantitatively confirm the results obtained by visual inspection. With the exception of the very small diameters, the particles show enhanced brightness at their edges, both at 1.5 kV (Fig. 2c) and 25 kV (Fig. 4c). Figure 3c shows a nearly constant brightness along the particle diameters, with a flat maximum at the centers. These effects also can be observed with other particle or substrate materials.

A substantial part of these particle size effects may be qualitatively explained in terms of the size of the interaction volume, compared to the particle diameters. A rough geometrical measure of the interaction volume can be given by the electron range R or the maximum information depth for backscattered electrons T, which is about one half of R ($T \approx R/2$). T strongly depends on the beam voltage (electron energy) according to the following equation (Reimer, 1985):

$$T = 2.8 \{(E^{1.54}) / \rho\} \text{ nm} \qquad (2)$$

The energy E of the incident primary electrons (PE) must be given in keV. ρ is the density of the material in g/cc. To simplify the discussion, we only consider spherical particles with a diameter of 40 nm; this roughly corresponds to the most probable value of particle size distribution. Corresponding to the experiments (results in Figs. 2, 3, and 4), we consider three different cases (beam voltage 1.5, 6, and 25 kV):

- For the low voltage (1.5 kV), T is about 10 nm which is small compared to the size of the particle. Those parts of the interaction volume that intersect the particle surface, and thus, can contribute to the emission of SE(1), BSE, and BSE produced SE(2), will be greater for a beam position at the particle edge than for a beam position at the top or center parts of the particle. If the particle and substrate materials give similar SE and BSE yields (both considered as bulk material), the image brightnesses of the particle center and the substrate will also be similar.
- At a medium beam voltage of 6 kV, the interaction depth T is about 60 nm. This is roughly in line with the considered particle diameter. With the PE beam at the center of the particle, almost the entire particle surface will contribute to the detected SE signal. Shifting the beam continuously to the rim of the particle, the emitting particle surface will slightly decrease with partial compensation by an increase in SE emitting parts of the substrate. As a result, the linescans across a particle will have a rather constant grey-value with a shallow maximum at the particle center. Using only a simple geometrical calculation, Seiler and Bauer (1989) have shown that a spherical particle can have a SE yield up to four times higher at its center compared to a flat substrate of the same elemental composition. In Figure

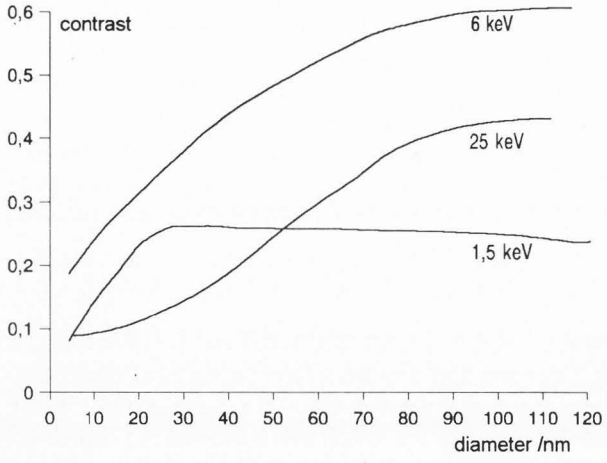

Figure 5a. Particle-to-substrate contrast as dependent on the particle diameter at three accelerating voltages.

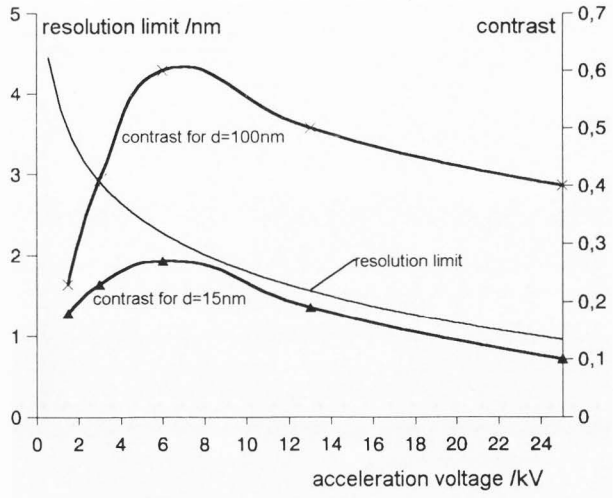

Figure 5b. Resolution limit and contrast (for two particle diameters) as dependent on accelerating voltage.

3b, as an example, the brightness of the particles with a diameter of 80 nm is higher by a factor of 3.6 than that of the substrate. Even for a substrate with a higher atomic number than that of the particles, the particles will always appear brighter (Ocker *et al.*, 1992b). The highest particle to substrate contrast is obtained at the beam voltage producing the best fit between the dimensions of the particle and the interaction volume.

- At a beam voltage of 25 kV, the interaction depth has grown to a size of almost 1 μm and its dominant part will be stretched down into the substrate. Nanometer sized particles will become visible by contrasts originating from a pure SE(1) signal, because the SE(2) and BSE contributions to the total detector signal only will show changes at a much lower spatial frequency (Joy, 1991). With the given conditions of a polished, structure-less substrate and a homogeneous layer of particles, the SE(2) and BSE will produce only a DC contribution to the video signal. As the PE beam, along its travel through the nanoparticle, will become broadened at most to a few nanometers, the SE(1) linescan across the particle diameter will show a variation similar to the well-known topographic contrast of conventional SEMs. A more detailed description of this effect must include SE that are produced (and also may be collected) at two additional sites of the PE trajectory: PE that hit the particle off its center will leave the particle on its rear side and finally penetrate the substrate. Such effects can strongly increase the edge SE yield and image brightness. If the particle and substrate materials have similar SE and BSE yields, the image brightness of the central particle area will again be similar to the substrate brightness. Moreover, with ever decreasing particle diameters, the edge effects of opposing parts of a particle will be superimposed (Joy, 1991). We observe this change of grey-value line profiles at a particle diameter of about 20 nm (Figs. 2c and 4c). This seems to be a direct consequence of the value of the maximal escape depth of SE in tin. Due to the lateral extension of the edge effect, an escape depth for SE of 10 nm corresponding to literature values (Seiler, 1983) can be estimated.

Summarizing the results of Figures 2b, 3b, and 4b, we have calculated the particle to substrate contrasts according to eq. (1). Figure 5a shows the regression curves at the three beam voltages 1.5 kV, 6 kV, and 25 kV as obtained for a common contrast scale. Again, it is evident that the medium beam voltage produces the highest contrasts. Figure 5b is another representation of Figure 5a. The contrasts are shown to be dependent on the beam voltage for two selected particle diameters. Figure 5b also shows the relation between the resolution limit of the HRSEM and the beam voltage, as can be coarsely estimated considering the corresponding spherical and chromatic lens aberrations. Combining these different influences to a measure for the image quality, we have calculated the ratio of contrast and resolution limit, obtaining an optimal beam voltage range between 10 kV and 15 kV. In other words: imaging such nanoparticulate matter at these beam voltages will yield a fairly good compromise between contrast and resolution.

Comparison of simultaneously acquired SE and TE micrographs

Figure 6a shows a scanning electron micrograph (at V_0 = 25 kV) of tin particles on carbon foil that was heated to a temperature of 150°C in the course of the

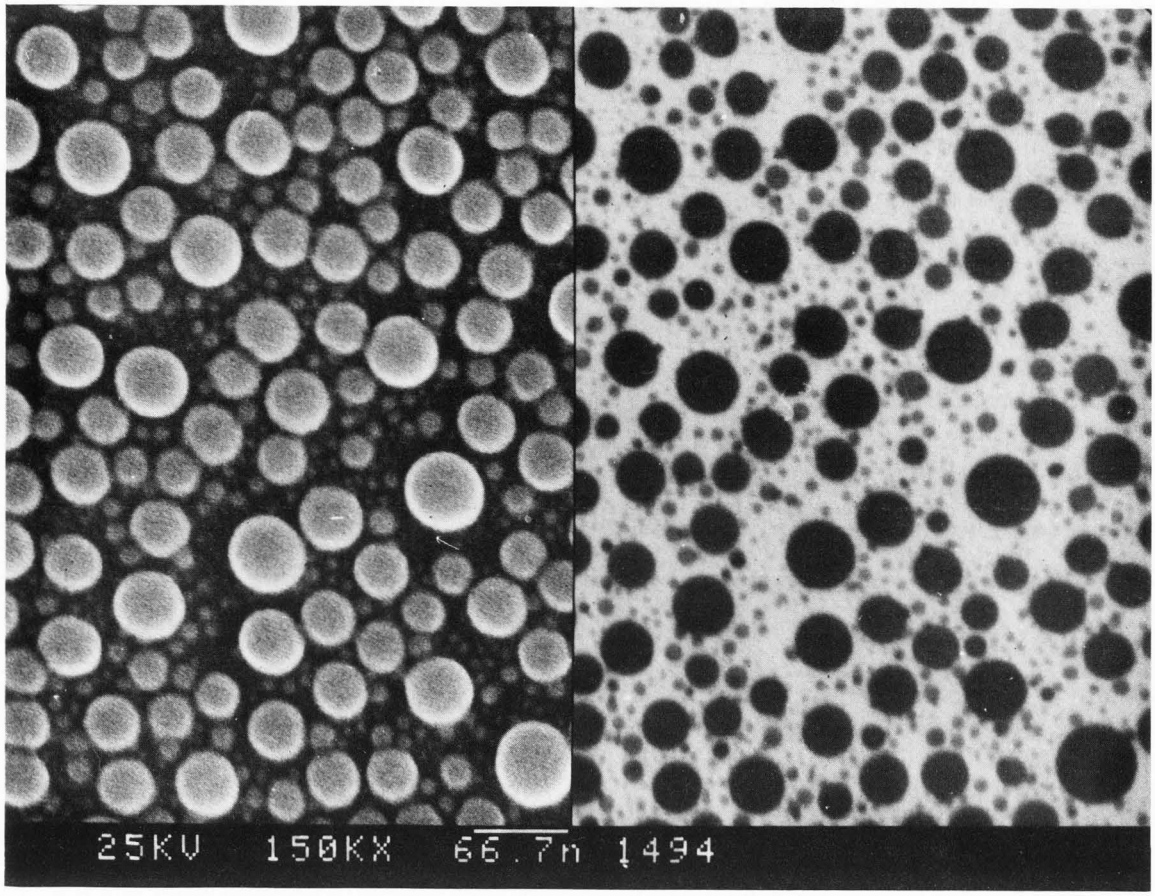

Figure 6a. Micrograph of tin particles on carbon foil at 25 kV: SE (left) and TE (right) signals. Bar = 66.7 nm.

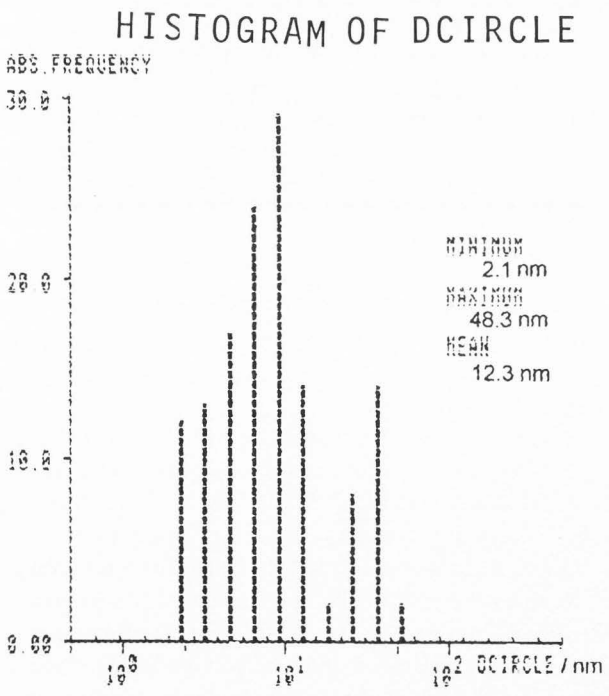

Figure 6b. Histogram of particle diameters SE mode.

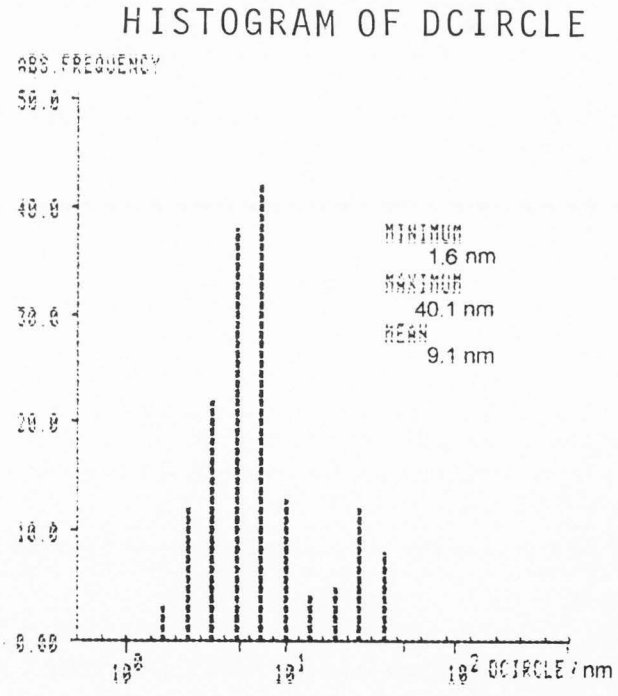

Figure 6c. Histogram of particle diameters TE mode.

evaporation. The deposited amount of tin is equivalent to a 20 nm thick homogeneous tin foil. The left side micrograph in Figure 6a corresponds to the SE signal, while the right side one has been obtained by collecting TE in the bright field mode. As both signals have been detected simultaneously, the two images represent exactly the same area of the specimen. Although the particles appear bright on a dark substrate and dark on a bright substrate for the SE and TE images, respectively, and thus, may misguide our visual perception, the particles appear to have smaller diameters in the TE micrograph. This impression becomes even more significant when considering the distances between the borders of neighboring particles. These distances appear larger in the TE image than in the SE image.

A careful inspection and analysis of the digital images clearly confirm what has been presumed by visual perception. Figures 6b and 6c show the histograms of the projected particle diameters for the SE and TE images, respectively. The particle diameters differ by about 3 nm for the smaller fraction of particles, but show deviations up to 8 nm for the largest particles. Size differences of the same order of magnitude have also been observed and measured for Ag- and In-particles, however, Au particles did not show this behaviour (results not shown).

One possible reason for this effect may be the excitation of plasmons (surface and/or bulk) by PE that pass the particle outside its projected area, but still within a certain distance. De-excitation of these plasmons has been proved to be another source of SE emission (Müllejans *et al.*, 1990, 1991). This type of delocalized SE generation will be of substantial influence, e.g., for the metals Sn, In, and Ag that have considerable cross-sections for plasmon excitations (especially, surface plasmons) in the energy range between 3 eV and 15 eV. This is well known from electron low energy loss spectra (ELELS) (Raether, 1980; Seiler *et al.*, 1991a,b). Assuming a threshold energy for the excitation of plasmons, one can calculate the utmost passing distance of PE in which the necessary energy and momentum transfer is possible (Howie and Milne, 1985). As an example, we get a distance of less than 10 nm in the case of 7 eV surface plasmons of tin when assuming a primary electron energy of 20 keV. As this value must be considered as an upper limit, the experimental increase of particle diameters is consistent with this theoretical estimate.

Conclusions

Metallic nanoparticles in the size range between 1 and 100 nm are most suitable for the testing of the performance of modern electron microscopes, e.g., the high resolution scanning electron microscope and the low voltage scanning electron microscope. Image quality in terms of contrast and resolution limit can be quantitatively assessed by an on-line operated digital image analyzer. Particle-to-substrate contrast and grey-value linescans strongly depend on the particle size and the beam voltage. The observed effects can be qualitatively interpreted on the basis of simple consideration of the geometrical size of the interaction volume (PE) and the information depths for SE and BSE emissions.

Using the power of the image analysis system, small differences between the particle diameters of SE and TE images clearly could be detected, providing another experimental evidence of delocalized plasmon induced SE emission.

Acknowledgement

This work was supported by a grant of the "Deutsche Forschungsgemeinschaft" (German science foundation).

References

Howie A, Milne RH (1985) Excitations at interfaces and small particles. Ultramicroscopy **18**, 427-434.

Joy DC (1991) The theory and practice of high-resolution scanning electron microscopy. Ultramicroscopy **37**, 216-233.

Kotera M, Fujiwara T, Yamaguchi S, Suga H (1993) Calculation of a topographic contrast in the scanning electron microscope. Scanning Microsc **7**, 547-554.

Lanio S, Frosien J, Drexel V, Weimer E (1993) A dedicated high resolution low voltage SEM. Optik **94**, Suppl. 5, 2 (abstract).

Müllejans H, Howie A, Bleloch A, McMullan D (1990) Coincidence measurements between energy loss and secondary electrons in STEM. In: MICRO'90. Elder HY (ed.). Royal Microscopical Society, Oxford, UK. pp. 39-42.

Müllejans H, Bleloch AL, Howie A, McMullan D (1991) Coincidences between secondary and energy loss electrons in STEM. Beitr. Elektronenmikroskop. Direktabb. Oberfl. **24**, 93-98.

Ocker B (1993) Untersuchung von Nanopartikeln mit Elektronen (Investigation of nanoparticles with electrons). Dissertationsschrift (Ph.D. Thesis), Inst. Physik, Univ. Hohenheim, Stuttgart, Germany. pp. 3-12.

Ocker B, Wurster R, Seiler H (1992a) Abbildung von Nanopartikeln im hochauflösenden und Niederspannungs-Rasterelektronenmikroskop (Imaging of nanoparticles in a high resolution and low voltage SEM). Proc. 15th Conf. of the Working Group "Scanning Microscopy in Materials Testing." DVM (Deuscher Verband für

Materialforschung), Berlin, Germany. pp. 265-274.

Ocker B, Wurster R, Seiler H (1992b) Image analysis of digitally recorded high resolution SE and BSE images. Beitr. Elektronenmikroskop. Direktabb. Oberfl. **25**, 111-114.

Raether H (1980) Excitation of Plasmons and Interband Transitions by Electrons. Springer Series in Optical Sciences **88**. Springer Verlag. pp. 45-59.

Reimer L (1985) Scanning Electron Microscopy. Springer Series in Optical Sciences **45**. Springer Verlag. pp. 128-142.

Seiler H (1983) Secondary electron emission in the scanning electron microscope. J Appl Phys **54** (11), R1-R18.

Seiler H, Bauer HE (1989) Einführung in die hochauflösende und die Niederspannungs-Rasterelektronen-Mikroskopie (Introduction in low-voltage and high resolution SEM). Beitr. Elektronenmikroskop. Direktabb. Oberfl. **22**, 1-10.

Seiler H, Haas U, Körtje K-H, Ocker, B (1991a) Investigation of metal cluster layers by EELS. Microsc Microanal Microstruct **2**, 191-201.

Seiler H, Haas U, Ocker B, Körtje K-H (1991b) Small metallic particles studied by optical and electron-optical spectroscopy. Faraday Discuss. **92**, 121-128.

Discussion with Reviewers

N.K. Tovey: You give an adequate and basic introduction to digital image acquisition. However, you omit any reference to exactly how you decided upon the threshold to segment the image, as presumably you must have done, into a binary form from which you could then derive the mean contrast within each particle. Even in the substrate, there will be a variation in the mean grey-value. Could you please indicate how you selected this threshold? Was it by manual selection, which can be notoriously unreliable, or by some specific algorithm (e.g., Watershedding, etc.)?

Authors: Discrimination between projected particle areas and the substrate is not easy to perform. We normally start this procedure by a program that allows interactive changing of the discriminating grey level and shows the resulting binary image overlaid with original one. From this qualitative inspection, it becomes clear whether shading and/or noise filtering programs must be applied. Subsequently, a non-linear two-dimensional delineation program sharpens the "grey-value steps" between particle and substrate, to be followed by the final discrimination. Although it is clear from critical dimension measurement discussions (e.g., Kotera *et al.*, 1993) that the site of a physically sharp edge and the brightness step do not necessarily correspond to each other, for want of a better knowledge, we have used these binary images for evaluation of particle dimensions and as a mask for densitometric measurements of the original image.

N.K. Tovey: Please indicate how you selected the area to determine GV_S. Are you sure you avoided areas which might have contained particles at the limit of resolution? How large were these areas? How much variation was there in the grey-values within these areas?

Authors: Dilating the final binary image (see above) to about twice its total area, then changing to its complementary image, we got a mask for measuring a reliable and representative set of grey values that covers about the same number of pixels as that of the accumulated area of all particles detected. Particles at and below the resolution limit only contribute a negligible amount to the substrate grey-value (see also Figs. 2b, 3b, and 4b). In support of this, we have measured the grey-value of particle free substrate areas for comparison.

N.K. Tovey: All three figures (2b, 3b, and 4b) show mean grey-values which are only slightly higher than the mean value of the substrate. Since there will always be a range in values in both particles and substrate, were difficulties encountered when selecting the threshold to avoid "holes" within the particles or odd small bright spots in the substrate? Perhaps it might be helpful to the reader if a typical binary segmented image could be shown.

Authors: As detailed in our answer (to the first question) above, prior to discrimination, original images have been processed to decrease the number and intensity of bright spots (a few pixels in size) or even to eliminate them entirely. Although the substrate is not atomically flat at all, this is no reason why bright spots should be there. Grey-value discrimination of particles with enhanced edge brightness produces holes within its binary image that are filled in by a special program. We have decided not to show a sequence of images produced by image processing and final discrimination because all what could have been demonstrated is exposed to the deterioration that comes from photographic and printing processes and can cause change and even loss of information.

N.K. Tovey: You say that the linescans (Figs. 2c, 3c, and 4c) are across the centers of some particles. I presume you mean that these were linescans across the whole image? If so, it would be helpful to the reader to indicate on the image where these linescans are, so that she/he can see the effects of the bright edges, etc. more clearly. Figure 4c also shows some very small peaks which could be manifestations of possible problems raised in the previous question.

Authors: The image analysis system (SEM-IPS) provides four different types of linescans to be extracted from a digital image by help of a menu driven software: horizontal linescan across the whole image, vertical linescan across the whole image, interactively pinned down polygonic linescan 500 points long (used in Figs. 2c, 3c, and 4c), and an interactively selected curved linescan 500 points in length. Small peaks seen in Figure 4c give an impression of the raw data/grey-values of the digital SEM images. How to deal with possible problems arising from it has been discussed in previous answers above.

N.K. Tovey: Could you please explain why the optimal beam voltage is between 10 and 15 kV? How does this reconcile with Figure 5?

Authors: In our SEM, we get the best SE resolution at $V_0 > 25$ kV; however, the highest particle-to-substrate contrast was obtained at $V_0 < 10$ kV. Our statement simply means this: One can get higher resolution only at the cost of reduced contrast and vice versa. Dividing the contrast curves of Figure 5b by a factor that corresponds to the course of the resolution limit, the maxima of these curves will shift to beam voltages of 10 kV and more.

M.-O. Delcourt: The resolution is claimed to be 1 nm. However, in Figures 2c, 3c, and 4c, such small particles cannot be seen. Analyses in Figures 2b, 3b, and 4b start from 4 nm.

Authors: There are two reasons why we have discarded measurements of particles less than 4 nm in diameter: (1) the decrease of particle grey-values with particle diameter ends up with a limit for automatically detecting collections of particles, because the excess brightness of the particle (compared to the substrate brightness) will become comparable to the standard deviation of mean substrate grey-values being measured in areas like those of the particles; and (2) although we can "see" particles of about 1 nm in diameter, particularly at magnifications of 200,000x and more, it becomes more difficult to determine the real borders of these spots by machine vision without having some knowledge of the corresponding point spread function.

There is experimental evidence for a resolution limit of 1 nm, e.g., in the linescans of Figure 4c, however. The lateral extension of the brightness steps at the particle borders (assumed to have rectangular shape) ranges between 1 and 3 nm, as 1 pixel corresponds to 1 nm. This is even more evident for linescans of TE images at 25 kV. Although questions concerning the resolution limit are very important, they are beyond the scope of this paper.

M.-O. Delcourt: The comparison of SE and TE signals show that the particle diameters are overestimated by 3 to 8 nm (Figs. 6b and 6c). This also is a limiting factor for the resolution.

Authors: We have to distinguish between accuracy and precision of a measurement. Overestimation of particle diameters by 3 to 8 nm clearly can be called poor accuracy. Distances between the particle boundaries will also be erroneous, whereas distances between centers of gravity would stay accurate. As to the precision (sharpness, resolution ...) of the particle edges, grey-value linescans across their rims should contain a wealth of information, particularly when compared to those of gold particles (no surface plasmon excitations). We have not performed such studies until now.

M.-O. Delcourt: From Figure 5a, the prediction for the best contrast is clearly 6 keV while the best experimental result is obtained for the lowest energy 1.5 keV. Please comment on this point.

Authors: You have compared the result of your visual perception of three photographs with the results of digital image analysis from three digital pictures (sets of digitized video signals). Therefore, you have to take into account all processes (electronic and photographic) that are involved in the transformation of a sequentially acquired video signal into a SEM image presented on photographic paper. Obviously, contrasts of the three photographs have been arbitrarily changed in the photo laboratory.

M. Kotera: The influence of the plasmon decay would not occur for insulating materials. Is it possible to do experiments for such materials to confirm the hypothesis?

Authors: Until now, we have not done this type of experiment for insulating particles. The idea is appealing, but two points should be reflected on: (1) insulating particles, e.g., MgO, do not show plasmon excitations, but similar to that show low energy excitations at their surfaces even if the electron beam passes outside the projected area of the particle (Howie and Milne, 1985); SE emission following the decay of these excitations cannot be excluded; and (2) surface and bulk charging of insulating specimens can heavily influence the imaging quality of SE-mode and even that of TE-mode, thus, probably confusing the interpretation of the results.

M. Kotera: Small particles have the smaller de-localization regions in themselves, how does this factor influence the signal intensity? The signal intensity decreases with size because of the volume to produce the signal. But how do the plasmon excitation and its decay influence the total intensity of the signal?

Authors: Unfortunately, we cannot separate SE according to the different types of interaction processes they are originating from. It should be possible to get more detailed information from overlaying SE- and TE-signal linescans about those SE that are produced by the PE passing the projected area of the particle. However, we do not have any model to extrapolate this contribution to the particle area/volume itself.

M. Kotera: If one collects only electrons with a little higher energy than the plasmon energy, can the image resolution be better than the normal secondary electron image?
Authors: SE collection combined with energy analysis or discrimination undoubtedly will give additional insights into that matter, but at the cost of reduced signal level. Also, our instrument is not equipped with any type of energy spectrometer. Electron energy loss spectrometry and electron spectroscopic imaging techniques, that are available in modern energy filtering transmission electron microscopes, may provide better capabilities.

R.H. Milne: When directly comparing the particle diameters observed in SE and TE modes, can you correlate the changes with the surface plasmon energies of the particles?
Authors: Until now, we have only compared the particle diameters of binary images obtained by discrimination of simultaneously acquired SE- and TE-images of particle collections. A more detailed analysis has shown the particle differences to vary monotonically with the actual particle diameter (approximately the one in the TE-image). So far no attempt has been made to overlay the corresponding linescans in getting more quantitative results as to the plasmon induced SE emission. A direct determination of surface plasmon energies would be desirable, but cannot be performed in our instrument. Alternatively, theoretical data, particularly those of how these energies depend on particle size could be used, if any reliable values do exist in the literature. To our knowledge, this is still a matter for debate because the physical properties of the particle's environment, e.g., an oxide layer can shift these energies too.

R.H. Milne: On samples with a high density of particles (e.g., Figure 6a), does shadowing affect the observed diameters in the SE images?
Authors: Shadowing effects can be very strong for SE-images acquired by means of an Everhart-Thornley detector. Shadow direction is opposite to the azimuthal site of the SE-detector. There is a quite different situation for SE detection and imaging of samples on an in-lens stage. Along the major part of their trajectories, SE are only influenced by the axial symmetric magnetic field of the objective lens. Let us consider two neighboring particles of about the same size at a distance (of their centers) smaller than twice the particle diameter. A great share of SE that are produced at the very rim of the particle will start with a take-off angle of zero. All those SE that are directed to a neighboring particle will have a good chance to be lost for detection. Careful inspection of Figure 6a reveals this kind of shadowing effect. However, the related brightness reductions are too small to create a detectable diameter decrease of the binary image at that point of the particle perimeter.

N.K. Tovey: In the second paragraph following eq. (2), your first sentence does not appear to agree with your figures. Could you please expand on this. The problem is that the grey-values for the 6 kV are consistently lower than the values for the lower voltage, despite your statement. Only at the largest diameters, does Figure 3b show higher values than Figure 2b.
Authors: You are correct if one compares the absolute grey-values as given in these figures. However, we have made a statement concerning the differences of grey-values (GV_p-GV_s) that seem to be consistently higher for 6 kV (Fig. 3b) than for the lower beam voltage 1.5 kV (Fig. 2b). The differences of the grey-values of particles and substrate, respectively, are important for the observation and contrast.